THE JOURNAL OF PHYSICAL CHEMISTRY B

ARTICLE

pubs.acs.org/JPCB

Transferable Force Field for Equilibrium and Transport Properties in Linear, Branched, and Bifunctional Amines I. Primary Amines

Gustavo A. Orozco,[†,‡] Carlos Nieto-Draghi,[†] Allan D. Mackie,[‡] and Véronique Lachet*[,†]

[†]IFP Energies nouvelles, 1-4 avenue de Bois-Préau, 92852 Rueil-Malmaison, France

[‡]Departament d'Enginyeria Química, ETSEQ, Universitat Rovira i Virgili, Av. dels Països Catalans 26, 43007 Tarragona, Spain

Supporting Information

ABSTRACT: A new anisotropic united atom (AUA4) force field is developed to predict the phase equilibrium and transport properties of different primary amines. The force field transferability was studied for an important set of molecules, including linear amines (methyl, ethyl, *n*-propyl, and *n*-hexylamine), branched amines (isopropyl and isobutylamine), and bifunctional amines (ethylenediamine, 1,3-propanediamine, and 1,5-pentanediamine). Monte Carlo simulations in the Gibbs ensemble were carried out to study thermodynamic properties such as equilibrium densities, vaporization enthalpies, and vapor pressures. Critical coordinates (critical density, critical temperature, and critical pressure) and normal boiling points were also calculated. The shear viscosity coefficients were studied for methyl, ethyl, and *n*-propylamine at different temperatures using molecular dynamics. Our results show a very good agreement with experimental values for thermodynamic properties and are an improvement on the models available in the literature, all of which are all-atom. Viscosity coefficients also show a good agreement compared with experimental data, demonstrating the transferability of our force field not only to predict thermodynamic properties but also to predict transport properties.

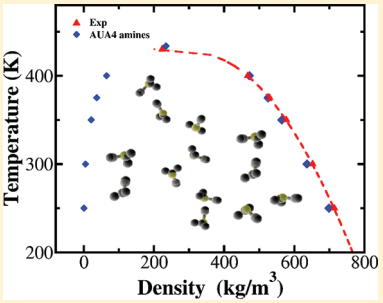

1. INTRODUCTION

Amines are used in several different industrial processes such as coal gasification, ammonia production, gas sweetening, and carbon dioxide capture. In the case of gas sweetening, extracted natural gas from oil fields is subjected to an industrial treatment where most of its contaminants are reduced to permitted levels. The components that need to be treated include acid gases, like CO_2 and H_2S among others. In recent years, the development of sweetening technologies has been of increased interest due to both economical and environmental reasons. In particular, the optimal design of processing units is crucial in order to improve the efficiency as well as the process yield. Furthermore, the correct design of the separation process units requires an accurate knowledge of the phase equilibria and also of the transport properties involved in it.

Different transferable force field approaches can be used to determine either transport properties, like viscosities, or thermodynamic properties, like vapor−liquid coexistence curves. One of the most popular approaches is the all-atom (AA) model, which assigns one force center (generally centered on its nucleus) to each atom in the molecule. A second approach is known as the united atom (UA) model, which assigns one force center for each chemical group in the molecule. A third approach, known as the anisotropic united atom (AUA), model introduces a displacement of the Lennard-Jones (L-J) force center of the UA model toward the hydrogens of the group. The AUA force field was originally proposed by Toxvaerd[1] and reparametrized by Ungerer[2] in a potential known as AUA4, which has shown good results for linear, branched, and cyclic hydrocarbons,[3−6] as well as for other functional groups such as alcohols,[7] ketones, and aldehydes,[8] sulfides, thiols,[9] and thiophenes.[10] One of the advantages of the AUA4 force field is first that the number of force centers is quite reduced compared with an AA model and second that vapor pressures and vaporization enthalpies have shown better results than other available models.

Several transferable force fields have been proposed in the literature to determine thermodynamic properties of amines using molecular simulation as an approach. One of the first, proposed in 1998 by Rizzo et al.,[11] follows the OPLS-AA (optimized potential for liquid simulations-all atom) philosophy, where they develop parameters for several amines, including 6, 8, and 10 partial charges for primary, secondary, and tertiary amines, respectively. The authors reported only one liquid density and one vaporization enthalpy at one temperature below the boiling point, which are in agreement with the corresponding experimental data for each studied amine. Several years later, another AA approach to study amines was proposed by Wick et al. in 2005[12] following the TraPPE-EH (transferable potential for phase equilibria-explicit hydrogens) philosophy. Wick concluded that the OPLS-AA liquid density agrees with experimental points close to its boiling point (267.2 K) but shows significantly larger deviations at elevated temperatures, reporting deviations higher than 10% for the critical temperature estimation. The same year, Boutard et al.[13] performed quantum chemistry and Monte

Received: August 8, 2011
Revised: October 21, 2011
Published: October 28, 2011

Carlo simulations in order to extend the AUA4 model to alkylamides and alkanols, and they also proposed a first attempt to model alkylamines. Four partial charges were defined for alkylamines with a different set for each molecule studied. Boutard's results for enthalpies of vaporization showed a reasonable agreement with experimental data, but there are important deviations in the calculated liquid densities (4−6%) and vapor pressures (40−60%). Due to the fact that hydrogens were not considered on the amine group, this model is not useful to study the hydrogen bond interactions both in pure systems and in mixtures. It is important to point out that for the specific case of amines, because they did not use the same set of charges for all of the studied molecules, there is a loss of transferability for the force field. Baskaya et al. (2005)[14] studied the vapor pressure and liquid density of 11 amines using discontinuous molecular dynamics simulations along with an adaptation of the UA approach and a discretized potential function. Overall average deviations for primary amines of 16% in vapor pressures are shown, but for ethylamine, they reported deviations of 31.7%. For the liquid densities, an overall deviation of 4.5% was found, but it is observed to increase with the chain length. Bauer et al.[15] studied methylamine, ethylamine, and *n*-propylamine in the condensed phase with charge equilibration force fields and molecular dynamics simulations in order to calculate radial distribution functions, dipole moment distributions, enthalpies of vaporization, isothermal compressibilities, diffusion constants, heat capacities, and other properties. Calculated volumes show discrepancies between 2 and 18% compared with experimental values, where the error increases with the size of the molecule. Enthalpy of vaporization and dielectric constant discrepancies are found to be in the range of 2.4−24.4% and 0.5−17.3%, respectively.

Among the models mentioned from the literature, the one that best reproduces the liquid−vapor methylamine equilibrium properties is the TraPPE-EH model. However, because it is an explicit hydrogen or AA model, when large molecules are simulated, the computing time is higher compared with a UA approach because the number of force centers is larger. Furthermore, because there are no L-J parameters on the hydrogens of the amine group and considering the fact that they have a charge, it is highly likely that two molecules can stick particularly in the case of molecules with a high dipole moment like alkanolamines or diamines. In addition, one of the disadvantages of the TraPPE-EH for amines, and in general for all of the available force fields, is that there is a lack of torsion parameters to extend the transferability study in a representative sample including linear, branched, and bifunctional amines. Finally, and equally important, although the TraPPE-EH model has a good agreement for the coexistence densities of methylamine, its deviations in vapor pressure are around 20%.

There is thus clearly a need to develop a UA force field that is able to predict the phase equilibrium properties for a larger set of amine molecules than the available AA models while attempting to maintain or even improve the agreement with experimental data. In this work, we propose an AUA model for primary amines that is able to meet these objectives. In the following section, details are given about the development of the force field as well as the six new torsions that have been developed for these molecules. In the Results section, a detailed description of the capabilities of the model is shown. In the final section, we finish with the main conclusions of this work.

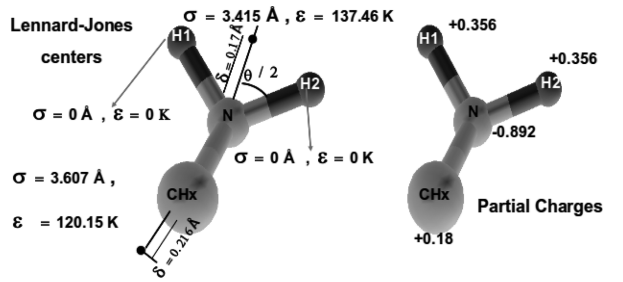

Figure 1. Schematic representation of AUA4 force field for amines. CH_x stands for CH_3, CH_2, or the CH group. L-J parameters given here are the ones of the CH_3 group.

2. FORCE FIELD DEVELOPMENT

2.1. Proposed Model and Nonbonded Interactions. Figure 1 represents our proposed AUA4 model for amines. As shown, four charges are proposed; two of them are located on the explicit hydrogens of the amine group (the hydrogens have no L-J interactions), one is on the nitrogen, and the last one is on the α-carbon atom of the anisotropic united methyl or methylene group. For the specific case of methylamine, two force centers were defined. The first one is located on the methyl group with a AUA displacement (δ), and the second one is located on the bisector of the HNH angle at a distance δ from the nitrogen. Hence, our model for amines has only three new parameters (σ, ϵ, δ) for the amine group. All other parameters are taken from the previous AUA4 model, along with the aforementioned charges.

Interactions between two force centers are calculated using a 12−6 L-J potential (eq 1), while electrostatic interactions are calculated using the Coulomb law (eq 2), where q_i and q_j represent the partial charges over the molecule and ϵ_o is the vacuum permittivity.

$$U^{L\text{-}J}(r_{ij}) = 4\epsilon\left[\left(\frac{\sigma_{ij}}{r_{ij}}\right)^{12} - \left(\frac{\sigma_{ij}}{r_{ij}}\right)^{6}\right] \quad (1)$$

Table 1. Nonbonded Parameters and L-J and Partial Charges

force center	ϵ (K)	σ (Å)	δ (Å)	$q(e)^a$	ref (L-J)
CH_3	120.15	3.607	0.216	+0.18 if bonded to N; 0 elsewhere	16
CH_2	86.29	3.461	0.384	+0.18 if bonded to N; 0 elsewhere	16
CH	50.98	3.363	0.646	+0.18 if bonded to N; 0 elsewhere	16
N	137.46	3.415	0.170	−0.892	this work
H(N)	0	0	0	+0.356	12

[a] The set of partial charges used in this work was taken from the TraPPE-EH force field, reported by Wick et al.[12]

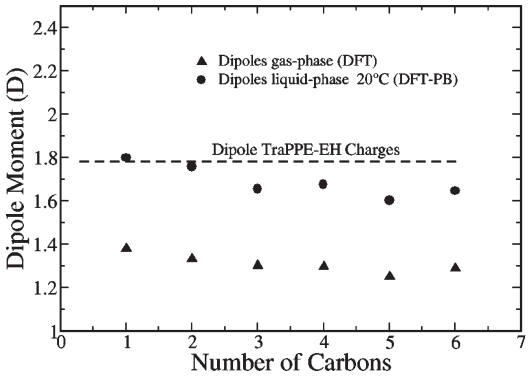

Figure 2. Comparison between gas and liquid dipole moments for the first six linear primary amines. Circles and triangles represent the dipole in the liquid and in the gas phase, respectively, and the dashed line corresponds to the dipole moment calculated using the TraPPE-EH charges.

$$U_{\text{Electrostatic}} = \frac{q_i q_j}{4\pi\epsilon_o r_{ij}} \tag{2}$$

Cross interactions were obtained using the Lorentz−Berthelot combining rules

$$\epsilon_{ij} = \sqrt{\epsilon_{ii}\epsilon_{jj}} \tag{3}$$

$$\sigma_{ij} = \frac{1}{2}(\sigma_{ii} + \sigma_{jj}) \tag{4}$$

The L-J parameters for the amine group were obtained through a numerical optimization, while all of the L-J parameters for carbons were taken from the AUA4 potential for hydrocarbons.[16]

Table 1 summarizes the nonbonded parameters used in our model.

2.1.1. Charges and Electrostatic Intermolecular Energy. To choose the set of charges for the amine group and the α-carbon, we first studied the dipole moment of a series of amines in the gas phase using density functional theory (DFT) at the B3LYP level, with 6-311G** as a basis set and using Jaguar[17] as the computational tool. The obtained results were compared with the numerical values available in the Computational Chemistry and Benchmarks Database of NIST,[18] finding excellent agreement with our values. The dipoles in the liquid phase were calculated using Jaguar's solvation model (Poisson−Boltzmann solver, PB) which fits the field produced by the solvent dielectric continuum to a set of point charges using experimental information[19−22] such as the dielectric constant, density, and molecular weight. Figure 2 shows the behavior of the dipole moment as a function of the number of carbons for the first six linear amines of the homologous series; triangles represent the dipole in the gas phase, circles are those in the liquid phase, and the dashed line represents the dipole moment using the TraPPE-EH charges for the most stable conformation. For all of the studied molecules, the calculated dipole in the liquid phase was between 28 and 31% higher than that in the gas phase, which is the usual behavior according to Tannor.[23] As we can see from this figure, there are only small variations in the dipole moment; hence, it can be considered to be constant, and consequently, a unique set of charges can be used to represent the behavior of all of the series. The TraPPE-EH set of charges overestimates on average the gas-phase dipole by 32% (see Figure 2), which justifies their choice in this work because they adequately reproduce the behavior of the dipole moment of the amines in the liquid phase.

It is important to mention that the TraPPE-EH set of charges is very similar to the charges in the OPLS-AA force field. The main difference between the two models is that in the OPLS-AA description, the charges of the α-methyl or methylene group are located on the hydrogens, whereas in TraPPE-EH, they are placed on the carbon. However, the total charge on the methyl or methylene group is the same in both models. Furthermore, the charges on the amine group are practically the same.

Table 2. Bond Lengths

bond	r_0 (Å)	ref
H−N	1.010	11
C−N	1.429	13
C−C	1.535	16

Table 3. Bending Parameters

angle	k_{bend} (K)	θ_0 (deg)	ref
CH_x−N−H	39642	109.50	11
H−N−H	47681	106.40	11
C−C−N	63630	109.47	11
CH_x−CH_2−CH_x	74900	114.00	16
CH_x−CH−CH_x	72700	112.00	16

2.2. Intramolecular Energy. All bonds were considered to be rigid. The C−N and N−H bond length values were taken from Boutard's work[13] and OPLS-AA for amines,[11] respectively. Other bond lengths were taken from the AUA4 force field for hydrocarbons.[2] Interactions between three connected atoms were modeled using a harmonic potential

$$U_{\text{bending}} = \frac{1}{2} k_{\text{bend}}(\cos\theta - \cos\theta_o)^2 \tag{5}$$

where k_{bend} is the bending constant and θ and θ_0 are the bending and equilibrium bending angles, respectively. Tables 2 and 3 summarize the bond lengths and bending parameters.

Interactions between four connected atoms were calculated as a function of the dihedral angle using the torsional potential given by eq 6, χ being defined such that $\chi = \phi + 180°$, where ϕ is the dihedral angle. The intramolecular energy for atoms separated by more that three bonds is computed using the same L-J potential as that in intermolecular interactions (eq 1). For bifunctional molecules, intramolecular electrostatic interactions were considered and calculated according to the local dipole approach proposed by Ferrando.[7] The main advantage using this approach is that it does not require additional interaction terms or scaling factors. Regarding the ethylenediamine molecule, because of the strong attraction between the two amine groups, an explicit 1−4 L-J intramolecular interaction was also considered.

$$U_{\text{tor}}(\chi) = \sum_{i=0}^{8} c_i[\cos(\chi)]^i \tag{6}$$

One of the most important aspects regarding the development of a force field is to check its transferability for different molecules. As we previously mentioned, one of the disadvantages of the TraPPE-EH force field for amines is that there exist only a limited number of available torsions, and this effectively restricts the molecules to which it can be applied. In our proposed force field,

Table 4. Calculated Torsions $E = \Sigma_i a_i \cos(\chi)^i$, All of Them Proposed in This Work

torsion	a_0	a_1	a_2	a_3	a_4	a_5	a_6	a_7	a_8
CH_x-CH_2-N-H	154.98	869.66	902.48	−586.25	−651.38	−607.86	253.22	149.74	102.90
$CH_x-CH_2-CH_2-N$	816.65	2509.94	9.01	−3609.00	−54.51	286.01	−104.22	−133.18	279.10
$CH_x-CH-CH_2-N$	546.87	1367.99	−26.97	−2344.08	−817.65	987.54	1163.02	−624.30	−340.10
$N-CH_2-CH_2-N$	1438.78	3531.87	−548.67	−3550.53	−1561.15	−1733.36	4323.74	933.26	−1997.11
$CH_x-CH-N-H$	60.65	238.22	218.52	−114.57	−353.18	−267.63	291.94	99.18	−71.84
CH_2-CH_2-CH-N	433.50	1189.15	113.34	−2030.74	646.72	530.37	−873.98	−414.92	520.52

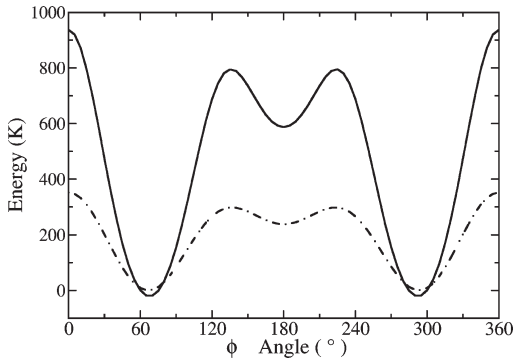

Figure 3. Comparison between the torsional energies for the CH_3-CH_2-N-H using the TraPPE-EH force field (dashed line) and the AUA4 force field (solid line).

different torsions were fitted in order to check its transferability to a large set of molecules, including linear, branched, and bifunctional amines.

In order to calculate the different torsion correlations for our force field, first of all, the total energy of the molecule in its ground state was calculated at different conformations between 0 and 360° of the dihedral angle ϕ. After that, and at each conformation, all of the other energy contributions such as bending energies, intramolecular L-J, intramolecular electrostatic interactions, and other torsional energies involving other dihedral angles were subtracted from the total energy obtained from a quantum calculation. Once the torsional energy was calculated at each conformation, the obtained values were fitted to a torsional potential using the analytical expression given by eq 6. Table 4 summarizes the coefficients after the fitting procedure. The total energy was computed at both DFT and a second-order Moller−Plesset perturbation theory (MP2), but there were no significant differences between the two calculations. Simulations were performed with Jaguar[17] software. For some of the studied molecules, it was possible to make a comparison with the values of the total energy reported in the literature,[24−27] finding excellent agreement. For ethylenediamine, the $N-CH_2-CH_2-N$ torsion was fitted according to the above exposed procedure. For this molecule, both L-J (including the 1−4 contribution) and intramolecular electrostatic interactions were considered and therefore subtracted from the total energy. The quantum calculation of the total energy was in excellent agreement with the one reported by Chang et al.[25,28] However, to the best of our knowledge, no torsions are available in the literature with which to compare.

Figure 3 shows the behavior of one of our fitted torsions as a function of the dihedral angle (ϕ) between 0 and 360° for the CH_3-CH_2-N-H torsion using ethylamine as a reference. The TraPPE-EH torsion is also shown. As we can see, there are three different minima corresponding to gauche (60°), anti (180°), and antigauche (300°) conformations. The differences between these two torsions are due to the fact that the TraPPE-EH force field is an AA potential, that is, all of the hydrogen atoms are considered in the molecule, meaning that an explicit account of H−C−C−H torsion and H−C−H bending is performed, explaining the observed differences between the two approaches.

2.3. Simulation Details. *2.3.1. Monte Carlo Simulations.* The Gibbs ensemble Monte Carlo method at constant volume and temperature was used to calculate the liquid−vapor equilibrium properties of the different studied amines for reduced temperatures in the range 0.6−0.9. In most cases, 40 million Monte Carlo steps (MCS) with an equilibration part between 1 and 10 million MCS were used, where one step corresponds to a single Monte Carlo move. Periodic boundary conditions and the minimum image convention were applied. A spherical cutoff equal to half of the simulation box was used to calculate the L-J interactions between force centers, and the Ewald procedure was used to handle the long-range electrostatic interactions,[31] with a maximum of seven vectors on each direction of the reciprocal space and a scaling parameter $\alpha = 2$ in reduced units. A total of 300 molecules were used for the simulations, except for at temperatures close to the critical point, where we increased the size of the system up to 600 molecules. The following Monte Carlo moves were used: translation (20%), rigid rotation (20%), configurational bias regrowth (20%), transfer with insertion bias (39.5%), and volume change (0.5%). For *n*-hexylamine, 1,3-propanediamine and 1,5-pentanediamine internal rotations (i.e., the rotation of a force center around its nearest neighbors) were also included in order to improve the sampling. The amplitude of translations, rotations, and volume changes was adjusted during the simulation to achieve an acceptance ratio of 40% for these moves. Note that for the temperature ranges considered in this study, that is, reduced temperatures greater than 0.6, transfer moves with configurational bias prove to be efficient to sample the phase equilibrium. If lower temperatures were to be considered, alternative methods to the Gibbs ensemble Monte Carlo could be used.[29,30]

The critical coordinates (critical density ρ_c and temperature T_c) were calculated through a scaling law (eq 7) and the law of rectilinear diameters (eq 8)

$$\rho_L - \rho_V = A(T_c - T)^{\beta^*} \tag{7}$$

$$\frac{\rho_L + \rho_V}{2} = \rho_c + B(T_c - T) \tag{8}$$

where β^* is a characteristic universal exponent (for this work, $\beta^* = 0.325$[31]) and ρ_L and ρ_V are the densities of the liquid and

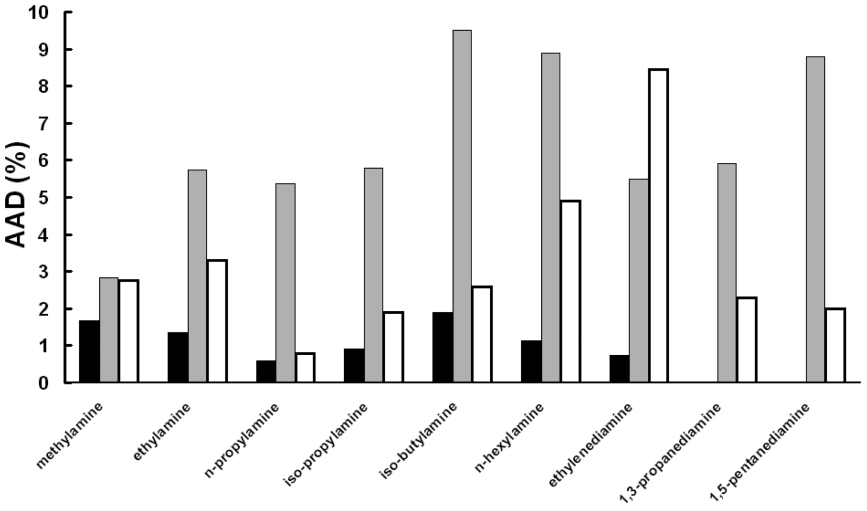

Figure 4. AAD obtained using the AUA4 potential for reduced temperatures between 0.6 and 0.9. Densities, vapor pressures, and vaporization enthalpies correspond to the black, gray, and white bars, respectively.

vapor phases, respectively. A and B are adjusted parameters. Normal boiling points (T_b) were estimated by fitting the vapor pressure (P_V) to the Clausius−Clapeyron equation (eq 9) at different temperatures, where C and D are constants. The simulations were performed using the in-house GIBBS Monte Carlo code developed by IFPEN and Orsay University.[16]

$$\ln P_V = \frac{C}{RT} + D \tag{9}$$

2.3.2. Molecular Dynamics. The equations of motion were integrated using the velocity Verlet algorithm with constrained bonds using the Rattle algorithm.[32] The simulations were performed in the *NPT* ensemble using both the Berendsen barostat and thermostat. Equilibration runs of 1 ns were used, while for the production part, 5 ns were applied. In both cases, the integration time step was 2 fs. A Verlet nearest-neighbor list was also included in order to improve the performance of the simulations. In all cases, 250 molecules were placed in a cubic box with periodic boundary conditions. To estimate the viscosity coefficients, we used both the Einstein and Green-Kubo formalisms. Calculations were performed using the Newton code developed at Orsay University. In order to calculate the viscosity coefficients, four different and independent initial configurations were used; hence, the values presented here correspond to the average of the obtained results for the four different configurations and its corresponding standard deviations.

2.3.3. Force Center Optimization. To optimize the L-J parameters, the procedure proposed by Bourasseau et al.[5] was followed. This is a minimum square method with an error criterion defined as eq 10

$$F = \frac{1}{n}\sum_{i=1}^{n}\frac{(X_i^{sim} - X_i^{exp})^2}{s_i^2} \tag{10}$$

where n is the total number of reference data, X_i^{sim} is the value obtained from the simulations, X_i^{exp} is the experimental data, and s_i is the uncertainty. F is an implicit function of σ, ϵ, and δ, which are the L-J parameters to be fitted. The overall idea is to minimize F with respect to these. In order to optimize the AUA L-J parameters, σ, ϵ, and δ, of nitrogen in the primary amines, three reference molecules were chosen, methyl, ethyl, and *n*-propylamine. Vaporization enthalpies, vapor pressures, and liquid densities were selected as the thermodynamic properties to be reproduced. For each molecule, two simulations were performed at two different temperatures, namely, 250 and 375 K for methylamine, 275 and 375 K for ethylamine, and 300 and 400 K for *n*-propylamine. For the statistical uncertainties, the values proposed by Bourasseau were chosen.[5] As initial guesses, we used the TraPPE-EH values for ϵ and σ, while for δ, the value proposed by Boutard was chosen.

3. RESULTS

Once the torsions were fitted, we proceeded to the optimization of the L-J parameters and then tested the transferability of our AUA4 force field for primary amines. A large set of molecules was chosen to test the new potential including methyl, ethyl, *n*-propyl, and *n*-hexylamine as linear molecules, isopropyl and isobutylamine as branched molecules, and ethylenediamine, 1,3-propanediamine, and 1,5-pentanediamine as bifunctional amines. In the following, we present the parameters obtained for our force field as well as its capability to predict thermodynamic properties such as liquid densities, vapor pressures, vaporization enthalpies, critical temperatures and densities, and normal boiling points. Finally, we present the viscosities obtained at different temperatures for methyl, ethyl, and *n*-propylamine.

3.1. Optimization and Transferability. After an iterative process, a set of optimized parameters for the nitrogen force center was found, with ϵ = 137.46 K, σ = 3.415 Å, and δ = 0.17 Å, which gives an error criterion (F in eq 10) of 0.97, which validates our numerical optimization. For the reference molecules at the temperatures mentioned before, a global average error was calculated for each property, obtaining 1.11% for the liquid densities (ρ_L), 3.87% for the vapor pressures (P_V), and 2.26% for the vaporization enthalpies (ΔH).

In order to check the transferability of our force field with the optimized parameters, different molecules were tested at different temperatures. A comparative table with all of the studied molecules, obtained numerical values, and corresponding errors and temperatures can be found in the Supporting Information.

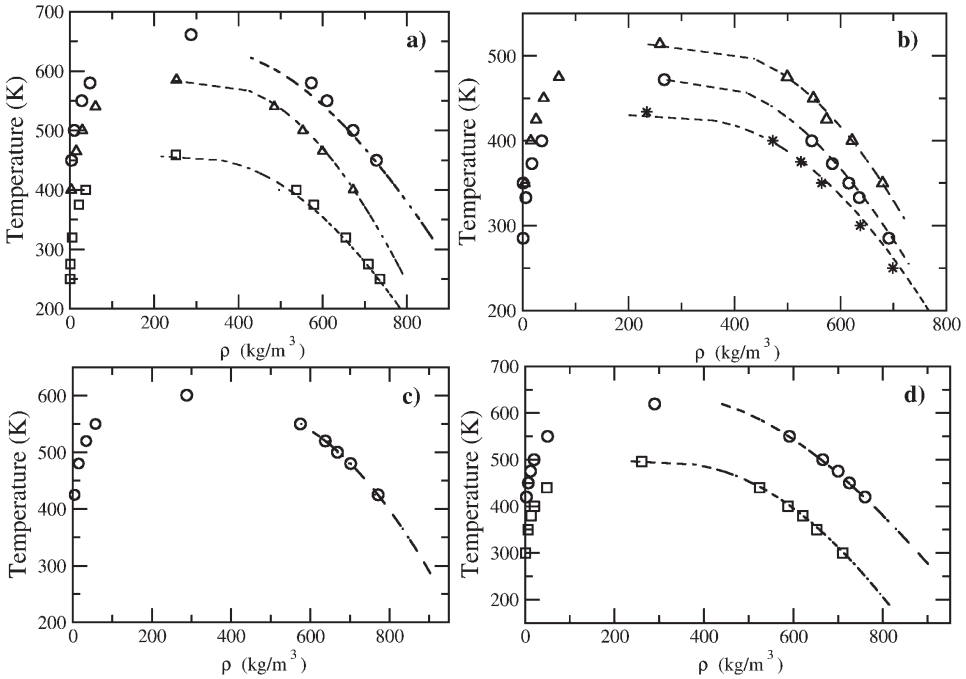

Figure 5. Comparison between experimental and simulated phase equilibrium diagrams. (a) Squares represent ethylamine, triangles *n*-hexylamine, and circles 1,5-pentanediamine. (b) Stars represent methylamine, circles isopropylamine, and triangles isobutylamine. (c) Ethylenediamine. (d) Squares represent *n*-propylamine and circles 1,3-propanediamine. In all cases, the dashed lines correspond to the DIPPR experimental correlations,[21] except for 1,5-pentanediamine and 1,3-propanediamine, where dashed lines are predicted values.

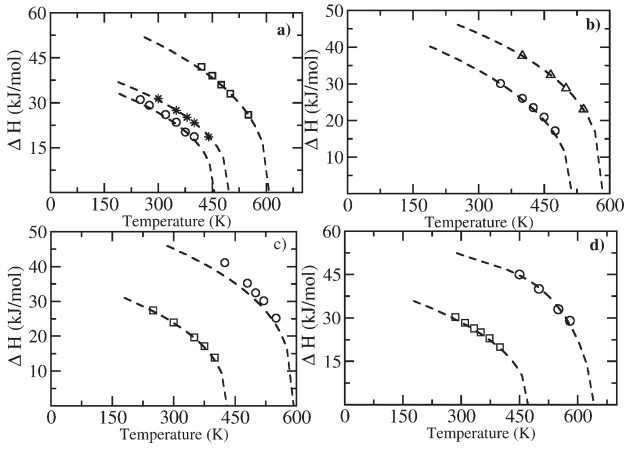

Figure 6. Comparison between experimental and simulated vaporization enthalpies. (a) Circles represent ethylamine, stars *n*-propylamine, and squares 1,5-pentanediamine. (b) Circles represent isobutylamine and triangles *n*-hexylamine. (c) Squares represent methylamine and circles ethylenediamine. (d) Squares represent isopropylamine and circles 1,3-propanediamine. In all cases, the dashed lines correspond to the DIPPR experimental correlations.[21]

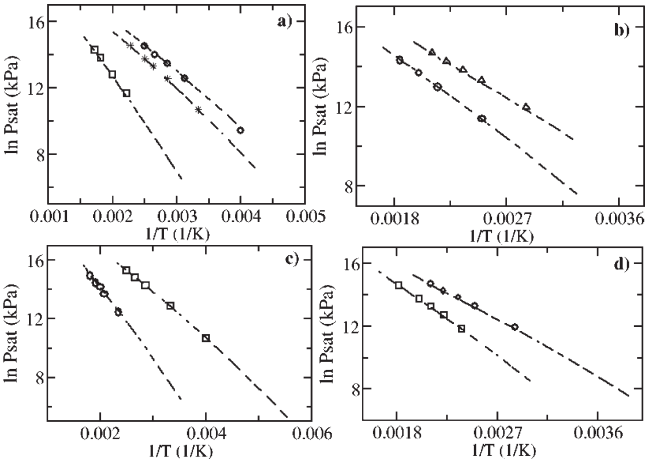

Figure 7. Comparison between experimental and simulated vapor pressures. (a) Circles represent ethylamine, stars *n*-propylamine, and circles 1,5-pentanediamine. (b) Circles represent *n*-hexylamine and triangles isobutylamine. (c) Circles represent ethylenediamine and squares methylamine. (d) Circles represent isobutylamine and squares 1,3-propanediamine. In all cases, the dashed lines correspond to the DIPPR experimental correlations.[21]

3.2. Thermodynamic Properties. As can be seen from Figure 4, the AUA4 force field for amines can be summarized as follows: for the studied linear amines, the obtained absolute average deviations (AAD = $|X^{exp} - X^{sim}|/X^{exp}$) were 1.2% for ρ_L, 5.0% for P_V, and 3.5% for ΔH. For the studied branched amines, the AAD were 1.4% for ρ_L, 7.6% for P_V, and 2.2% for ΔH. Finally, for the studied bifunctional molecules, experimental information was found only for vapor pressures and vaporization enthalpies, leading to a global error of 6.2% for P_V and 4.3% for ΔH. With regard to experimental information for densities, there was only data available for ethylenediamine, showing excellent agreement with our simulation results of an AAD of 0.9%. Comparison of our calculated liquid densities for 1,3-propanediamine and 1,5-pentanediamine was done against predicted data from the DIPPR database. These are predicted values using the Racket equation,[21] and for this reason, AAD is not reported.

Table 5. Critical Coordinates and Normal Boiling Points, Comparison between Experimental and AUA4 Values

	T_c (K)			ρ_c (kg/m^3)			P_c (kPa)			T_b (K)		
molecule	exp	sim	AAD%	exp	sim	AAD%	exp	dim	AAD%	exp	sim	AAD%
MA	430.8	433_3	0.7	232	234_3	0.6	7460	7564_{34}	1.4	266.8	269_2	0.9
EA	456.0	458_2	0.7	244.0	251_5	3.1	5620	6056_{42}	7.8	289.7	294_3	1.5
iso-PA	471.8	469_3	0.2	267.5	265_4	0.6	5582	5590_{38}	0.1	304.1	304_1	0.3
PA	496.9	495_2	0.2	na	260_5		4740	5645_{62}	19	321.0	319_2	0.4
iso-BA	513[a]	513_2	0.04	na	259_4		4215[a]	4283_{51}	1.6	335.6	340_2	1.5
HA	584.0[a]	584_2	0.7	na	252_2		3180[a]	3204_{35}	0.7	405.8	405_1	0.1
ED	593.0[a]	600_3	1.1	na	288_2		6459[a]	6290_{32}	2.7	390.4	392_2	0.5
1,3-PDA	632.0 ± 6[b]	619_3	1.1	na	289_2		5120[a]	6130_{37}	19.7	410.1	407_2	0.8
1,5-PDA	na	661_4		na	287_2		3735[a]	4969_{28}	33.0	447.5	451_1	0.8

[a] Predicted values taken from DIPPR (method of Lydersen). [b] Experimental value taken from ref 33; na = not available. MA = methylamine, EA = ethylamine, iso-PA = isopropylamine, PA = *n*-propylamine, iso-BA = isobutylamine, HA = *n*-hexylamine, ED = ethylenediamine, 1,3-PDA = 1,3-propanediamine, and 1,5-PDA = 1,5-pentanediamine. For ethylamine, experimental values were taken from ref 34. The subscripts give the statistical uncertainties of the last digit(s).

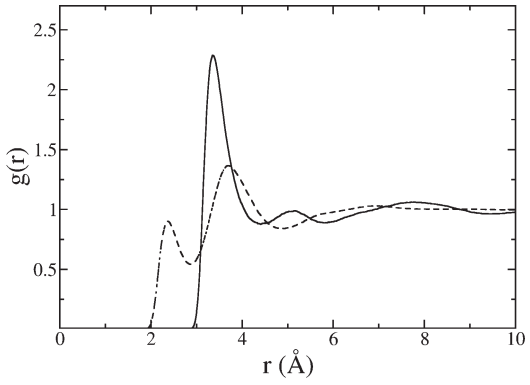

Figure 8. Radial distribution functions for methylamine. Solid and dashed lines represent g_{N-N} and g_{N-H} respectively.

For all of the studied molecules, the calculated liquid−vapor phase diagrams are given in Figure 5, the vaporization enthalpies are in Figure 6, and the vapor pressures are in Figure 7.

3.3. Critical Points and Normal Boiling Points. Table 5 shows a comparison between experimental[21,34] and calculated normal boiling points, critical temperatures, critical densities, and critical pressures. Normal boiling points (T_b) have been calculated using the Clausius−Clapeyron equation. We want to emphasize the fact that for both critical temperatures and critical pressures, only some experimental data are available to compare with; these include methylamine, ethylamine, and isopropylamine; additionally for critical temperatures, there is also experimental data for propylamine. Other values reported in Table 5 correspond to predicted values. For other molecules, we compare our results with the calculated critical values given by the TraPPE-EH model. As can be seen, the predictions of critical coordinates are in excellent agreement with the experimental data with deviations less than 1% for the estimation of the critical temperature. The critical density predictions are also better than the ones reported for the TraPPE-EH force field (ρ_c = 252 and 257 kg/m^3 for methyl and ethylamine, respectively). With regards to the DIPPR predicted critical pressures, it is important to mention that their corresponding uncertanties are between 10 and 25%, and there is no TraPPE-EH value available with which to compare. Concerning the normal boiling points, the biggest errors were for ethylamine and isobutylamine at around 1.5%, which reflects again the accuracy of the AUA4 model for amines.

3.4. Structure of the Liquid Phase. Figure 8 shows both the N−N and N−H radial distribution functions (rdf) for methylamine obtained with our force field at 230 K and 1 bar. This temperature was chosen because there is some experimental information about distances and coordination numbers for pure methylamine obtained by neutron diffraction and reported by Hayama et al.[35] Considering the N−N rdf, the first peak was found around 3.3 Å, yielding a coordination number of 4.4. These results are in agreement with the simulated values reported by Kusalik et al.[36] at 250 K (peak location at 3.0 Å and coordination number of 4) and by Feng et al.[37] at 203 K (peak location at 3.1 Å and coordination number ranging between 3.61 and 4.08). With regards to the N−H rdf, two peaks were found around 2.3 and 3.6 Å. The first one that corresponds presumably to the hydrogen bonding agrees very well with the experimental value (2.30 ± 0.01). The second one, around 3.6 Å, corresponds to nonbonded hydrogens and is in good agreement with the simulated values reported by Kusalik (3.3 Å) and more recently by Feng (3.3 Å) at 203 K and 10 MPa. Integrating over the first peak yields a coordination number of 1.1, very close to the one obtained by Kusalik (∼1.0) and in very good agreement with the experimental value reported by Hayama (1.0 ± 0.3). The peak positions for N−C and C−C rdfs (not shown) were also in very good agreement with Hayama's experimental values.

Despite the absence of a formal definition for hydrogen bonding, different criteria have been proposed in the literature, either considering the energy or the geometry between the involved atoms.[38,39] In the present study, we used a geometric criterion that considers the distance between two nitrogen atoms N and N′. Similar criteria have already been applied for alcohols and amines.[7,37] The N−N′ distance was defined by taking into account the first solvation shell of the N−N′ pair distribution function. We obtained on average two hydrogen bonds per methylamine molecule. This number of hydrogen bonds is much less than the coordination number, suggesting a low degree of hydrogen bonding in the first solvation shell. Such behavior was already reported by Feng and Kusalik.

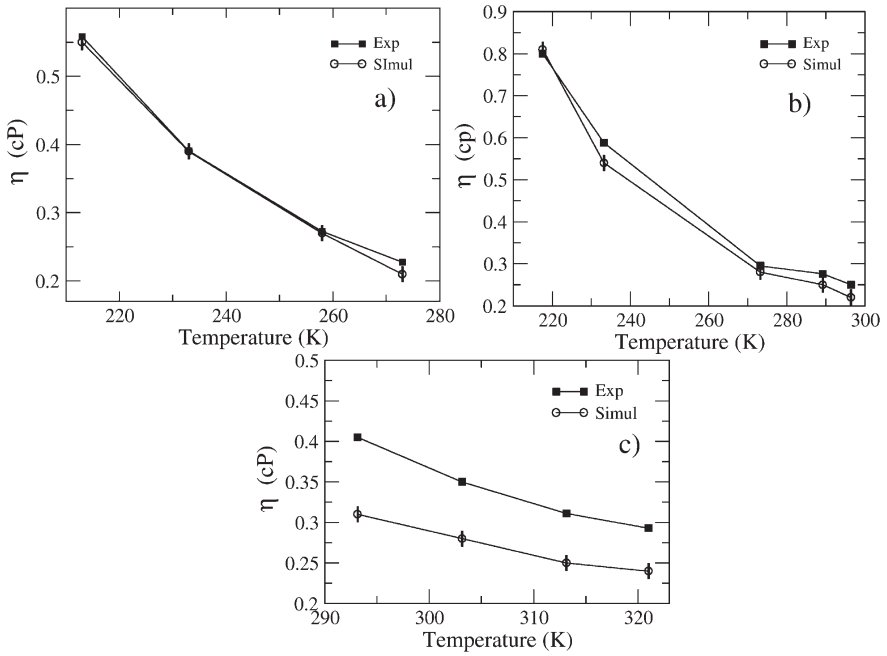

Figure 9. Shear viscosities as a function of temperature, (a) methylamine, (b) ethylamine, and (c) *n*-propylamine.

Table 6. Methylamine, Ethylamine, and *n*-Propylamine Viscosity Coefficients in cP[a]

		viscosities (cP)		
molecule	temperature (K)	exp	simul EF	simul GKF
methylamine	213.00	0.5584	0.55 ± 0.03	0.56 ± 0.02
	233.00	0.3909	0.39 ± 0.02	0.41 ± 0.01
	258.00	0.2726	0.27 ± 0.01	0.27 ± 0.03
	273.00	0.2275	0.21 ± 0.02	0.24 ± 0.02
ethylamine	217.50	0.800	0.81 ± 0.01	0.84 ± 0.02
	233.20	0.588	0.54 ± 0.01	0.54 ± 0.01
	273.20	0.299	0.28 ± 0.01	0.28 ± 0.01
	289.20	0.276	0.24 ± 0.01	0.25 ± 0.01
	296.40	0.250	0.21 ± 0.01	0.22 ± 0.01
n-propylamine	293.15	0.405	0.31 ± 0.01	0.32 ± 0.01
	303.15	0.350	0.28 ± 0.01	0.28 ± 0.01
	313.15	0.311	0.25 ± 0.01	0.25 ± 0.01
	321.00	0.293	0.24 ± 0.01	0.23 ± 0.01

[a] EF = Einstein formalism; GKF = Green-Kubo formalism.

3.5. Viscosity Coefficients. Figure 9 shows a comparison between the experimental (squares) and simulated (circles) viscosity coefficients at different temperatures. Three molecules were studied, methyl, ethyl, and *n*-propylamine. Numerical values are also shown in Table 6. As expected, for all of the simulated molecules, the results using Green-Kubo and Einstein formalisms are the same taking into account the statistical uncertainty. Compared with experimental values,[21,40−43] the agreement is excellent for methylamine and ethylamine, with global errors of 1 and 6%, respectively. For *n*-propylamine, the agreement is reasonable, with an average deviation of 18%. These deviations are consistent with the reported values using the AUA4 potential for *n*-alkanes, where for ethane and *n*-pentane, the obtained AAD were 8.16 and 33.52%, respectively.[44]

4. CONCLUSIONS AND PROSPECTS

Our proposed AUA4 model for primary amines is a force field based on the AUA approximation with only one force center per functional group. Nevertheless, we obtain an excellent precision for densities, vaporization enthalpies, and vapor pressures as compared to experimental data. With respect to the estimation of the critical coordinates and normal boiling points, the same excellent accuracy was obtained for the critical temperatures and normal boiling points as compared with the TraPPE-EH model, and in addition, the critical densities are better estimated using AUA4.

Thanks to the different torsions fitted in this work, it was possible to demonstrate the transferability of the AUA4 force field over a large set of primary amines including linear, branched, and bifunctional molecules. Other transferable force fields, such as OPLS-AA and TraPPE-EH, are restricted in that sense due to a lack of available torsions. It is worth mentioning that this is the first time that a force field is also tested for bifunctional and branched amines. As we have shown, our simulation results are again in excellent agreement with the experimental values for all studied molecules. In the case of the structure of the liquid phase, our force field presents a good agreement with previous simulation works and also with the available experimental information.

Finally, the viscosity coefficients calculated from the molecular dynamics simulations show a very good agreement with the experimental values for the studied amines at different temperatures. This demonstrates that the AUA4 model is able not only to predict thermodynamic properties but also transport properties.

Further work is in progress to extend the AUA4 model to secondary and tertiary amines.

■ ASSOCIATED CONTENT

Supporting Information. Simulation results and experimental values of saturated liquid densities, vaporization enthalpies, and vapor pressures are given for all of the studied molecules

at different temperatures. This material is available free of charge via the Internet at http://pubs.acs.org.

AUTHOR INFORMATION

Corresponding Author
*E-mail: veronique.lachet@ifpen.fr.

ACKNOWLEDGMENT

The authors would like to thank Dr. Bernard Rousseau for the use of the Newton MD code. A.D.M. acknowledges financial help from the Spanish Ministry of Science and Innovation MICINN via Project CTQ2008-06469/PPQ.

REFERENCES

(1) Toxvaerd, S. *J. Chem. Phys.* **1990**, *93*, 4290–4295.
(2) Ungerer, P.; Beauvais, C.; Delhommelle, J.; Boutin, A.; Rousseau, B.; Fuchs, A. H. *J. Chem. Phys.* **2000**, *112*, 5499–5510.
(3) Mackie, A. D.; Tavitian, B.; Boutin, A.; Fuchs, A. H. *Mol. Simul.* **1997**, *19*, 1–15.
(4) Nieto-Draghi, C.; Bocahut, A.; Creton, B.; Have, P.; Ghoufi, A.; Wender, A.; Boutin, A.; Rousseau, B.; Normand, L. *Mol. Simul.* **2008**, *34* (2), 211–230.
(5) Bourasseau, E.; Haboudou, M.; Boutin, A.; Fuchs, A. H.; Ungerer, P. *J. Chem. Phys.* **2003**, *118*, 3020–3034.
(6) Bourasseau, E.; Ungerer, P.; Boutin, A. *J. Phys. Chem. B* **2002**, *106*, 5483–5491.
(7) Ferrando, N.; Lachet, V.; Teuler, J. M.; Boutin, A. *J. Phys. Chem. B* **2009**, *113*, 5985–5995.
(8) Ferrando, N.; Lachet, V.; Boutin, A. *J. Phys. Chem. B* **2009**, *114*, 8680–8688.
(9) Delhommelle, J.; Tschirwitz, C.; Ungerer, P.; Granucci, G.; Millie, P.; Pattou, D.; Fuchs, A. H. *J. Chem. Phys.* **2000**, *104*, 4745–4753.
(10) Pérez-Pellitero, J.; Ungerer, P.; Mackie, A. D. *J. Phys. Chem. B* **2007**, *111*, 4460–4466.
(11) Rizzo, R. C.; Jorgensen, W. L. *J. Am. Chem. Soc.* **1999**, *121*, 4827–4836.
(12) Wick, C. D.; Stubbs, J. M.; Neeraj, R.; Siepmann, J. I. *J. Phys. Chem. B* **2005**, *109*, 18974–18982.
(13) Boutard, Y.; Ungerer, P.; Teuler, J. M.; Ahunbay, M.; Sabater, S.; Pérez-Pellitero, J.; Mackie, A.; Bourasseau, E. *Fluid Phase Equilib.* **2005**, *236*, 25–41.
(14) Baskaya, F. S.; Gray, N. H.; Gerek, Z. N.; Elliot, J. R. *Fluid Phase Equilib.* **2005**, *236*, 42–52.
(15) Bauer, B. A.; Patel, S. *J. Mol. Liq.* **2008**, *142*, 32–40.
(16) Ungerer, P.; Tavitian, B.; Boutin, A. *Applications of molecular simulation in the Oil and Gas Industry*; Technip: Paris, 2005; p 267.
(17) *Jaguar*, version 7.7; Schrodinger, LLC: New York, 2010.
(18) http://cccbdb.nist.gov/dipole2.asp (Jan 2011).
(19) Cronenwett, W.; Hoogendoorn, L. W. *J. Chem. Data* **1972**, *17*, 298–300.
(20) McClellan, A. *Table of experimental dipole moments*; W. H. Freeman and Co.: New York, 1963; Vol. I—III.
(21) Rowley, R.; Wilding, W. L.; Oscarson, J. L.; Danner, R. P. *Design Institute for Physical Properties*; AIChE: New York, 1987.
(22) Ghosh, P. N.; Chatterjee, T. P. *Phys. Rev.* **1931**, *37*, 427–429.
(23) Tannor, D. J.; Marten, B.; Murphy, B.; Friesner, R. A. *J. Am. Chem. Soc.* **1994**, *116*, 11875–11882.
(24) Batista de Carvalho, L. A. E.; Texeira-Dias, J. J. C.; Fausto, R. *Struct. Chem.* **1990**, *1*, 533–542.
(25) Chang, Y.; Su, T. *J. Mol. Struct.* **1996**, *365*, 183–200.
(26) Chen, K.; Lii, J.; Fan, Y.; Allinger, N. *J. Comput. Chem.* **2007**, *28*, 183–190.
(27) Maxwell, D. S.; Tirado, R. J.; Jorgensen, W. L. *J. Comput. Chem.* **1995**, *16*, 984–1010.
(28) Chang, Y.; Su, T.; Li, T.; Chao, I. *J. Phys. Chem. A* **1997**, *101*, 6107–6117.
(29) Desgranges, C.; Delhommelle, J. *J. Chem. Phys.* **2009**, *130*, 244109–244116.
(30) Aleksandrov, T.; Desgranges, C.; Delhommelle, J. *Fluid Phase Equilib.* **2010**, *287*, 79–83.
(31) Frenkel, D.; Smit, B. *Understanding molecular simulations*; Academic Press: New York, 2002; p 201.
(32) Andersen, H. *J. Chem. Phys.* **1983**, *52*, 24–34.
(33) Nikitin, E. D.; Popov, A. P. *J. Chem. Eng. Data* **2006**, *61*, 609–611.
(34) Lixiong, L.; Kiran, E. *J. Chem. Eng. Data* **1988**, *33*, 342–344.
(35) Hayama, S.; Wasse, J. C.; Skipper, N. T.; Walters, J. K. *Mol. Phys.* **2001**, *99*, 779–786.
(36) Kusalik, P. G.; Bergman, D.; Laaksonen, A. *J. Chem. Phys.* **2000**, *113*, 8036–8046.
(37) Feng, H.; Liu, X.; Gao, W.; Chen, X.; Wang, J.; Chen, L.; Ludemann, H. D. *Phys. Chem. Chem. Phys.* **2010**, *12*, 15007–15017.
(38) Jorgensen, W. L.; Ibrahim, M. *J. Am. Chem. Soc.* **1982**, *104*, 373–378.
(39) Jorgensen, W. L. *J. Am. Chem. Soc.* **1981**, *103*, 335–340.
(40) Shah, J. K.; Dewitt, K. J.; Stoops, C. E. *J. Chem. Eng. Data* **1969**, *14*, 333–335.
(41) Dye, J. L.; Dalton, L. R. *J. Phys. Chem.* **1967**, *71*, 184.
(42) Makhija, R. C.; Stairs, R. A. *Can. J. Chem.* **1970**, *48*, 1214–1218.
(43) Campbell, A. N.; Lam, Y. *Can. J. Chem.* **1973**, *51*, 4005–4008.
(44) Nieto-Draghi, C.; Ungerer, P.; Rousseau, B. *J. Chem. Phys.* **2006**, *125*, 1–15.